JOURNAL OF APPLIED ELECTROCHEMISTRY 23 (1993) 352–357

Oxygen reduction on stainless steel

R. BABIĆ, M. METIKOŠ-HUKOVIĆ

Institute of Electrochemistry, Faculty of Technology, University of Zagreb, Zagreb, Croatia

Received 8 May 1992; revised 5 September 1992

Oxygen reduction was studied on AISI 304 stainless steel in 0.5 M NaCl solution at pH values ranging from 4 to 10. A rotating disc electrode was employed. It was found that oxygen reduction is under mixed activation–diffusion control. The reaction order with respect to oxygen was found to be one. The values of the Tafel slope depend on the potential scan direction and pH of the solution, and range from -115 to $-180\,\mathrm{mV\,dec^{-1}}$. The apparent number of electrons exchanged was calculated to be four, indicating the absence of H_2O_2 formation.

Nomenclature

B $= 0.62\,nFcD^{2/3}\nu^{-1/6}$
c bulk concentration of dissolved oxygen ($\mathrm{mol\,dm^{-3}}$)
D molecular diffusion coefficient of oxygen ($\mathrm{cm^2\,s^{-1}}$)
E electrode potential (V)
E_H^0 standard electrode potential (V)
F Faraday constant ($96\,500\,\mathrm{A\,s\,mol^{-1}}$)
I current (A)
j current density ($\mathrm{A\,cm^{-2}}$)
j_k kinetic current density ($\mathrm{A\,cm^{-2}}$)
j_L limiting current density ($\mathrm{A\,cm^{-2}}$)
m reaction order with respect to dissolved oxygen molecule
M molar mass ($\mathrm{g\,mol^{-1}}$)
n number of transferred electrons per molecule oxygen
ρ density ($\mathrm{g\,cm^{-3}}$)
ν kinematic viscosity ($\mathrm{cm^2\,s^{-1}}$)
ω angular velocity ($\mathrm{s^{-1}}$)

1. Introduction

The electrochemical reduction of oxygen has attracted a great deal of interest in recent years especially due to the industrial development of fuel cells, its possible use in the chlor-alkali industry and its role in the corrosion of metals and alloys [1].

The corrosive process of almost all technically significant metals and alloys in an almost neutral solution takes place with oxygen depolarization. In general, the oxygen electroreduction can take place directly to OH^-, to OH^- via H_2O_2 formation and to H_2O_2 as a final reduction product, as follows:

$$O_2 + 2H_2O + 4e^- \longrightarrow 4OH^- \qquad E_H^0 = 0.401\,V \qquad (1)$$

$$O_2 + H_2O + 2e^- \longrightarrow HO_2^- + OH^- \qquad E_H^0 = -0.0649\,V \qquad (2)$$

$$HO_2^- + H_2O + 2e^- \longrightarrow 3OH^- \qquad E_H^0 = 0.867\,V \qquad (3)$$

Thus it is possible to observe a four-electron pathway, a two-electron pathway as well as a number of electrons between two and four.

Excellent review papers concerning oxygen reduction on various kinds of electrode material, and the proposed mechanisms, have been published [1–3]. Here, only the investigations of oxygen reduction on iron and steel electrodes will be mentioned. Generally, the electrochemical reduction of oxygen on iron and steel, as well as other technical metals and alloys, has been poorly investigated. It depends a great deal on the state of the electrode surface, which can be influenced by many factors which makes the elucidation of reaction mechanism rather tedious. This is probably the reason why few papers have been devoted to the study of oxygen reduction on iron and steels in near neutral solution.

In a neutral phosphate solution, Delahay [4] found a four-electron pathway on a bare iron surface, while at a more positive potential he also observed the formation of H_2O_2. In a borate buffer solution (pH 7–10), Jovancicevic and Bockris [5] found a four-electron pathway with a little H_2O_2 on a bare iron surface, while oxygen reduction on a passive surface is terminated at the H_2O_2 stage. In a near neutral borate and bicarbonate buffer, Drazic *et al.* [6–8] found the four-electron pathway at all potentials, but due to a very small rate of H_2O_2 formation with respect to the total reduction current, a reliable distinction between the parallel and series mechanism could not be made [7]. These authors also observed [8] an inhibiting effect due to the formation of a nonconductive film in the reaction of H_2O_2 and Fe(II) ions. The inhibiting effect is not observed when the iron dissolution rate is small. Calvo and Schiffrin [9] found that oxygen reduction on passive iron in alkaline solutions is much more irreversible than on platinum, and occurs only in the potential range where the passive film is reduced. The reaction order with respect to oxygen was 0.5 and the Tafel slope was $-140\,\mathrm{mV\,dec^{-1}}$.

0021-891X

The electrochemical reduction of oxygen on an iron electrode in almost neutral solutions containing chloride ions has been investigated by Drazic *et al.* [10, 11]. They found a four-electron pathway which suggests that oxygen is reduced completely to OH^-. They observed that the Tafel slope is higher in unbuffered (-150 to $-180\,mV\,dec^{-1}$) than in buffered NaCl solution (about $-120\,mV\,dec^{-1}$).

The electroreduction of oxygen on steel electrodes in neutral chloride solutions has also been investigated. Wroblowa and Qaderi [12] found that the mechanism of oxygen reduction at a low carbon steel surface in alkaline solutions is relatively simple in that direct four-electron reduction, reoxidation and chemical decomposition of peroxyl ions are absent. The limiting currents for a two and four-electron (sequential) reduction are very well defined. On a passive steel surface, Wroblowa and Qaderi found a stable peroxyl ion as the only product. Kuznetcov and Nelaev [13] found that in a 0.5 M KCl solution the reaction takes place simultaneously via a two-electron and four-electron pathway and that the amount of H_2O_2 increases with the potential change in the cathodic direction. Bonnel *et al.* [14] found, on a steel electrode in a 3% NaCl solution at -915 mV, a four-electron reduction of oxygen.

The electrochemical reduction of oxygen on 316 stainless steel in a 0.5 M NaCl solution has been investigated by Muralidharan *et al.* [15]. They found a four-electron pathway, a reaction order with respect to oxygen of nearly 1 at -0.7 V, and a Tafel slope between -125 and $-130\,mV\,dec^{-1}$.

The present work has been performed to gain more information about the mechanism of oxygen reduction on a stainless steel electrode in a 0.5 M NaCl solution of pH from 4 to 10.

2. Experimental details

The steel sample selected for the study had the following composition by percent weight: C, 0.106; Si, 0.93; Mn, 1.40; P, 0.030; S, 0.010; Cr, 18.17; Ni, 9.03; Mo, 0.017. Disc electrodes suitable for the EG&G PARC Model 616 system were machined from a cylindrical rod with a cross sectional area of 1 cm^2. The electrodes for other polarization measurements were cut from a cylindrical rod with a cross section of 0.5 cm^2. Pieces 5 mm long, with electrical contact made by a brass screw, were axially embedded by Araldite into glass holders giving a circular exposed geometric area of 0.5 cm^2. The counter electrode was a platinum gauze and the reference electrode was a saturated calomel electrode (SCE). All potentials are referred to the SCE. The electrode surface was mechanically polished with a fine grained emery paper followed with 0.3 μm alumina-water suspension on a polishing cloth to obtain a mirror surface. After this, the electrodes were washed with distilled water, then with ethanol and finally rinsed with triply distilled water. In order to reduce the air-formed oxide, the electrode was, prior to each experiment, subjected to a cathodic pretreatment by holding potentiostatically at -1.1 V for 10 min.

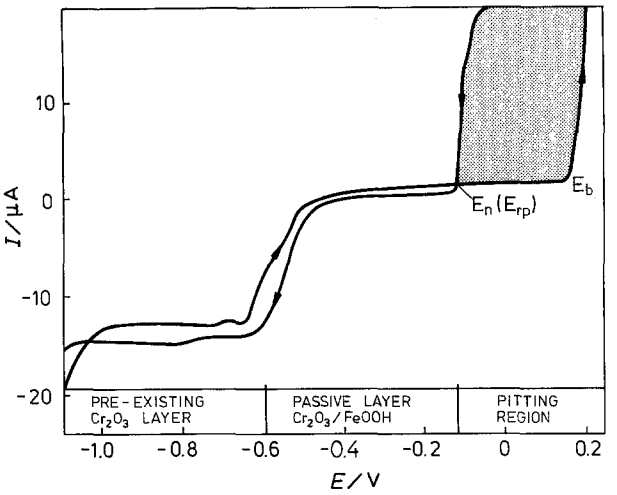

Fig. 1. Polarization curve for a stainless steel electrode in aerated 0.5 M NaCl pH 10 solution recorded in the denoted direction at a sweep rate of 0.5 mV s^{-1}.

Measurements were performed in a 0.5 M NaCl solution of pH 4–10. The adjustment of pH was made by ammonium hydroxide and hydrochloric acid. Prior to the experiments in inert atmosphere, the electrolyte was deaerated by passing pure nitrogen for 3 h through it and thereafter above it.

Polarization measurements with an RDE were carried out in an EG&G cell (50 ml). The measurements with stationary electrodes were performed in a glass cell (200 ml) with a separate compartment for the reference electrode connected with the main compartment via a Luggin capillary. Both cells were a water-jacketed version, connected to a constant temperature (20 ± 0.05 °C) circulator.

The polarization E against I curves were obained by means of the linear potential sweep technique with sweep rates ranging from 0.5 to 20 mV s^{-1}. The potentiostat was an Amel Model Metalloscan.

Results and discussion

3.1. *Polarization measurements with a stationary electrode*

To obtain a general picture of the behaviour of the investigated stainless steel electrode in a near neutral 0.5 M NaCl solution, potentiodynamic measurements with a slow sweep rate (0.5 mV s^{-1}) were carried out. The polarization started from -1.1 V in the anodic direction until the electrode had been activated and was then reversed with the same sweep rate. The results obtained in all solutions of pH between 4 and 10 were almost alike, and a typical E against I curve is shown in Fig. 1. In the potential range examined, there are three distinct regions: the limiting current region and a passive region followed by a pitting region.

The change from cathodic to anodic current takes place without the activation–passivation transition. The typical activation maximum that appears during

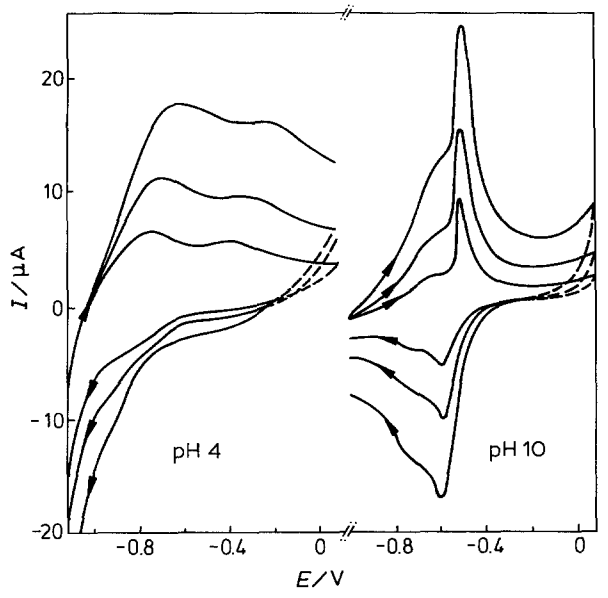

Fig. 2. Voltammograms for a stainless steel electrode in nitrogen saturated 0.5 M NaCl solution at (a) pH 4 and (b) pH 10. Scan rates: 20, 10 and 5 mV s^{-1}.

the active/passive transition on iron and nickel is not present here. In the case of 304 stainless steel [16], as well as in the case of chromium [17], even brief contact of the electrode with moist air is sufficient to create a thin oxide layer on the surface of the electrode. This explains the absence of an activation maximum on the *E–I* curves. Current increase starts at the breakdown potential, E_b, continuing even after the potential scan reversal. The hysteresis loop thus obtained allows the pit nucleation potential, E_n, to be determined [18]. E_n is denoted as the potential below which no pitting occurs, and above which pit nucleation starts. In this sense, it can be regarded as the protection or repassivation potential, E_{rp} [19].

To investigate the state of the steel surface on which the oxygen reduction takes place, polarization measurements in deaerated solutions were made. Cyclic voltammograms with a sweep rate of 5, 10 and 20 mV s^{-1} were performed. Although the main characteristics of the voltammograms are almost the same, their shape continuously changed with increase in pH. This can be seen in Fig. 2, where the voltammograms obtained at pH 4 and 10 are presented.

In the anodic part of the voltammograms two current maxima can always be distinguished. With increase in sweep rate these are shifted in the anodic direction in solutions of pH ranging from 4 to 8. In a solution of pH 10 the position of the current maxima are independent of sweep rate. The decrease in the anodic current related to the achievement of full passivation takes place at approx. −0.1 V in a slightly acid solution and −0.3 V in a slightly alkaline solution.

The first peak can be assigned to the electroformation of the hydrous $Fe(OH)_2$ layer which is electrooxidised to a hydrous FeOOH layer at the potential of the second current peak [20–23]. The electroformation of Fe(II) and Fe(III) layers takes place according to Ramasubramanian *et al.* [23] and Konig and Schultze [24] on a preexisting Cr_2O_3 layer which cannot be electroreduced. By the formation of an outer hydrous FeOOH rich layer on an inner Cr_2O_3 rich layer, a stable passive state is achieved.

On the cathodic part of the cyclic voltammograms it is also possible, in many cases, to distinguish two current peaks that can be assigned to the reduction of anodically formed oxide species. From Fig. 2 it can be seen that the electroreduction of iron oxide species ceases at potentials between −0.8 and −0.9 V.

Ellipsometric investigations performed by Matsuda *et al.* [25] showed that the process of passivation of 18–8 stainless steel in NaCl solution takes place in the potential range −0.6 to −0.2 V and that a stable passive state exists up to 0.1 V. According to these authors the passive film at −0.2 V is about 1.2 nm thick and, with increasing potential up to 0.1 V, its thickness increases up to 1.8 nm. The thickness of the passive film on 304 [26] and 316 stainless steel [27] in a 3% NaCl solution was calculated from capacity data amounted to 2 to 3 nm, depending on the applied potential. From potentiostatic *I* against *t* transients [27] the film thickness on 316 stainless steel in 3% NaCl solution was calculated to be 1.4 nm relating to Fe_2O_3 and 2.6 nm relating to $Fe(OH)_3$, respectively.

The amount of charge during the anodic polarization calculated from the obtained voltammograms (Fig. 2) depends slightly on the sweep rate and is about 15% less at 20 mV s^{-1} than at 5 mV s^{-1}. The value obtained ranges from 1.6 to 2.1 mC cm^{-2} regardless of pH. Assuming the formation of FeOOH (M = 88 g mol^{-1} and ρ = 3 g cm^{-3}) the above amount of charge corresponds to a film thickness of 1.6 to 2.1 nm. On the assumption of a Fe_2O_3 formation (M = 159.7 g mol^{-1} and ρ = 5.6 g cm^{-3}) the film thickness would be 0.85 to 1.1 nm. The potentiostatic measurements performed in this research show that the same amount of charge is consumed during the polarization of the electrode for 10 min at a potential of −0.1 V and that a film thickness of 0.9 to 1.1 nm can be calculated. By decreasing the potential of polarization, the amount of charge decreases and at −0.3 V it is approx. half of the value obtained at −0.1 V.

Comparing the obtained voltammograms with the *E* against *I* curve obtained in the air saturated solution (Fig. 1) it may be observed that the oxygen reduction at high current densities takes place on the reduced electrode surface. In the potential range where the current plateau exists the electrode surface is covered only by a thin (about 1 nm thick) layer of chromium-rich oxide [23], which exhibits, as in the case of chromium passivation [28], significant electronic conductivity.

3.2. *Polarization measurements with a RDE*

The polarization curves were obtained by linear potential sweep technique with a sweep rate of 5, 10 and 20 mV s^{-1} and with a rotation rate ranging from

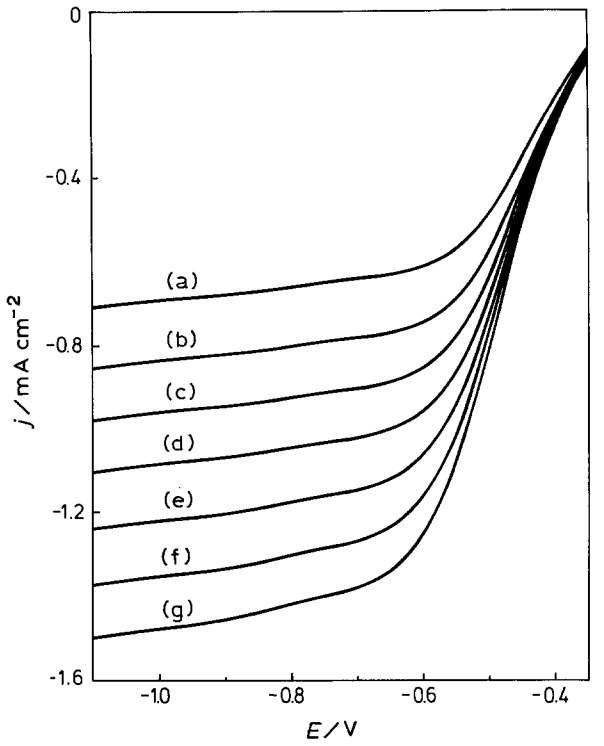

Fig. 3. Polarization curves for oxygen reduction in 0.5 M NaCl pH 4 solution recorded in anodic direction at a scan rate 10 mV s^{-1}. Specified rotation rates: (a) 1000, (b) 1500, (c) 2000, (d) 2500, (e) 3000, (f) 3500 and (g) 4000 r.p.m.

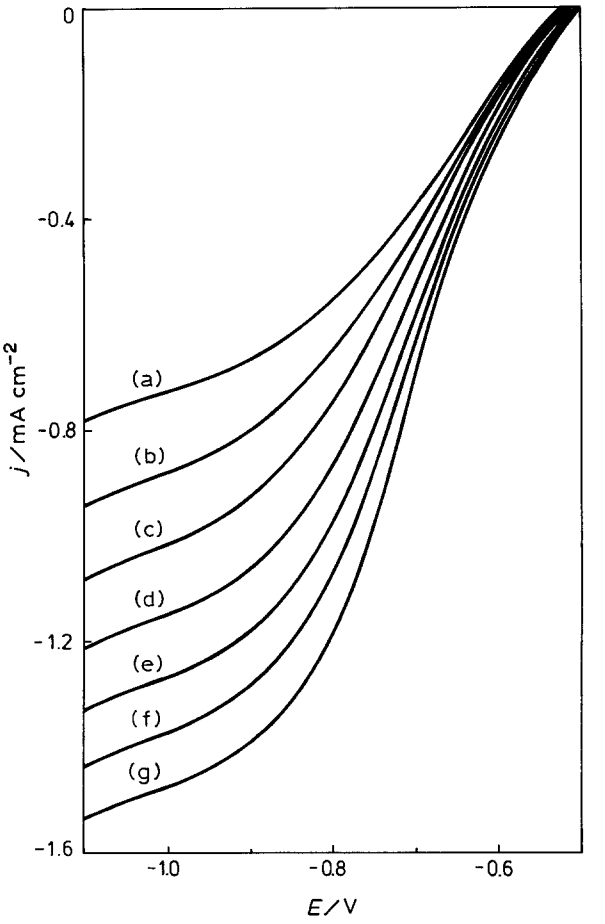

Fig. 4. Polarization curves for oxygen reduction in 0.5 M NaCl pH 10 solution recorded in anodic direction at a scan rate 10 mV s^{-1} at specified rotation rates as for Fig. 3.

1000 to 4000 r.p.m. in steps of 500 r.p.m. In all experiments the potential sweep started from −1.1 V and went in the anodic direction until the current zero and then in a reverse direction.

The curves obtained are very similar in shape. For example, the sets of curves obtained at pH 4 and 10 are presented in Fig. 3 and Fig. 4. It is evident, as in other cases, that the curves obtained are of S-shape with expressed limiting plateau dependent on a rotation rate. The S-shape of curves is better expressed in almost neutral solutions than in slightly alkaline or acid ones. For instance, the current value of 0.1 mA was achieved during a course of polarization of about 150 to 200 mV in almost neutral solutions, while only for about 50 mV in a slightly alkaline or acid solution.

The well defined S-shaped curves and the dependence of the reduction current on rotation rate indicate that the process is under mixed activation–diffusion control at all rotation rates examined. According to these characteristics analysis of the results obtained has been made.

3.2.1. Limiting current. The appearance of limiting current dependent on the rotation rate suggest their comparison with those calculated on the basis of Levich equation:

$$j_L = 0.62nFcD^{2/3}v^{-1/6}\omega^{1/2} \quad (4)$$

where n is the number of transferred electrons per oxygen molecule, F the Faraday constant, c the bulk concentration of dissolved oxygen, D the molecular diffusion coefficient of oxygen, v the kinematic viscosity, and ω the angular velocity.

The following set of values for 0.5 M NaCl solution at 20 °C [14]: c, 2×10^{-7} mol cm^{-3}; D, 1.74×10^{-5} cm^2 s^{-1}; v, 10^{-2} cm^2 s^{-1} gives a slope of j_L against $\omega^{1/2}$ plot equal to 69.3 μA cm^2 $s^{-1/2}$ for $n = 4$, which is presented in Fig. 5 by the solid line. The average limiting current at each rotation rate calculated from $24E$ against j recordings (at pH 4, 6, 8 and 10 and sweep rate 5, 10 and 20 mV s^{-1} in the anodic and reverse scan direction) is almost exactly on the theoretical line, as can be seen from Fig. 5. This fairly good agreement between the experimental and calculated values indicates that a four-electron reduction takes place. This means that in the region of high current densities oxygen is probably completely reduced to OH^-. However, the slope of the j_L against $\omega^{1/2}$ relationship depends very much on the accuracy of diffusivity and oxygen solubility data. The four-electron reduction of oxygen has also been found in the case of 316 stainless steel in 0.5 M NaCl solution [15].

3.3.2. The reaction order with respect to O_2. The reaction order can be determined from the slope of the plot

$$\log j = \log j_k + m \log(1 - j/j_L) \quad (5)$$

where j_k is the kinetic current density and m is the reaction order with respect to dissolved oxygen molecules.

The values of current j at all rotation rates were

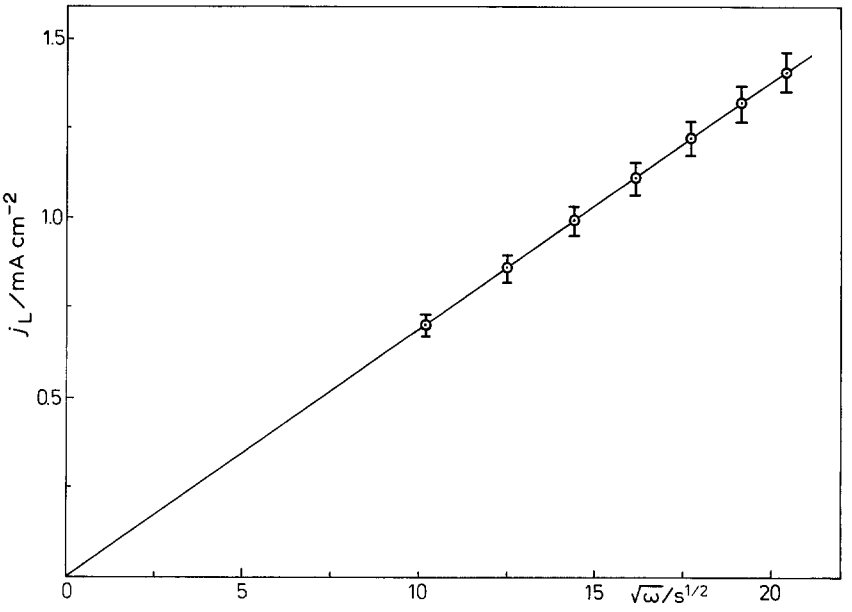

Fig. 5. Dependence of limiting current of oxygen reduction on angular velocity. Solid line: calculated for $n = 4$. The experimental values are the average of 24 E–j measurements.

chosen at potentials ranging from -525 to -700 mV depending on the solution pH value. In all cases the plot $\log j$ against $\log(1 - j/j_L)$ gave a fairly good straight line, as shown in Fig. 6. The slopes were mostly between 0.98 and 1.04 and very rarely up to 1.08, suggesting a first order reaction.

For the first order reaction with respect to dissolved oxygen, the observed disc current is related to the rotation rate by the equation [29]

$$1/j = 1/j_k + B^{-1}\omega^{-1/2} \quad (6)$$

where B is the so-called Levich slope, and according to Equation 4, is equal to $0.62nFcD^{2/3}\nu^{-1/6}$.

Figure 7 shows a plot $1/j$ against $\omega^{-1/2}$ obtained from experimental data in 0.5 M NaCl solution pH 6. Similar plots are also obtained for the solution with other pH values. The linearity and parallelism in these plots confirm that the kinetics are first order with respect to oxygen. The experimental values of B mostly range from 0.069 to 0.08 mA cm^{-2} min$^{1/2}$, and are in good agreement with the calculated value according to Equation 4 ($B = 0.069$ mA cm^{-2} min$^{1/2}$). A satisfactory agreement between these two values can be taken as evidence of four-electron reduction of oxygen on a steel electrode in a near neutral 0.5 M NaCl solution.

3.2.3. Tafel slopes. Tafel slopes were determined from the plot of E against $\log[j/(j_L - j)]$. In all cases a straight line was observed over one decade of current, and with slope from -115 to -180 mV dec^{-1}, as shown in Fig. 8.

The Tafel slopes obtained in the anodic scan direction were always lower than those in the reverse scan direction, and they do not exceed the value

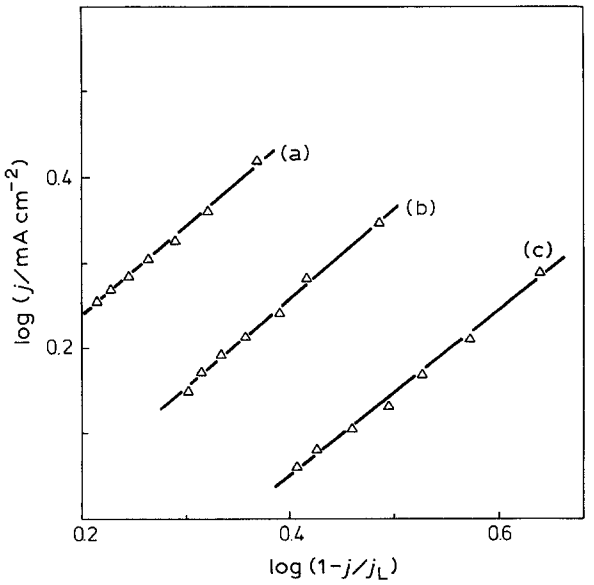

Fig. 6. Dependence $\log j$ against $\log(1 - j/j_L)$ for oxygen reduction in 0.5 M NaCl pH 4 solution at specified potentials: (a) -0.475, (b) -0.500, and (c) -0.525 V.

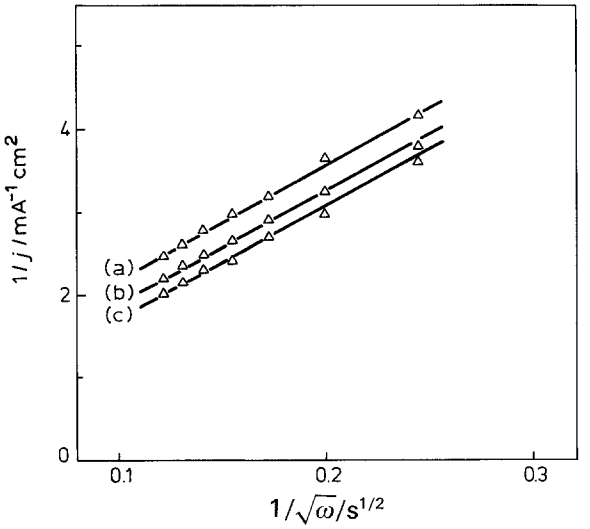

Fig. 7. Dependence $1/j$ against $\omega^{-1/2}$ for oxygen reduction in 0.5 M NaCl pH 6 solution at specified potentials: (a) -0.500, (b) -0.515, and (c) -0.525 V.

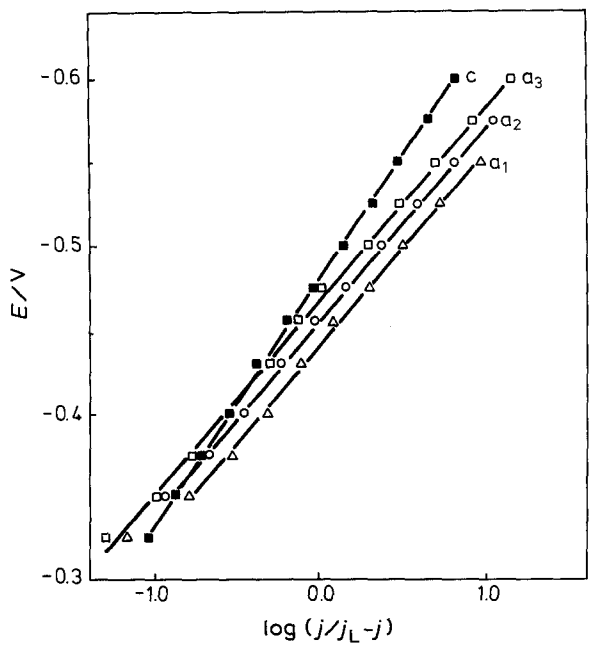

Fig. 8. Tafel plots for oxygen reduction in 0.5 M NaCl pH 4 solution obtained for: (c) cathodic and (a) anodic scan direction at specified rotation rates: (△) 1000, (○) 2000, (□) 2500, and (■) 2500 r.p.m.

of $-155\,mV\,dec^{-1}$ at higher pH. At pH 4 Tafel slopes of -115 to $-120\,mV\,dec^{-1}$ were found. All these findings are in accordance with literature data [11, 15, 27, 30].

The influence of solution pH, as well as scan direction, on Tafel slopes may be connected with the state of the electrode surface. Comparing the E against I curves obtained in a nitrogen saturated solution (Fig. 2) with those obtained in air saturated solution (Fig. 3 and Fig. 4) it can be seen that the Tafel line lies in the potential range where the electrode is not covered only by a Cr_2O_3 rich layer. In this potential range, according to voltammograms in Fig. 2, the formation of iron (II) and iron (III) intermediate species is possible. It is known that values of the Tafel slope ranging from -120 to $-200\,mV\,dec^{-1}$ are often observed in reactions through adsorbed layers at a metal surface, while the thicker layers of oxide cause a further increase of the slope up to $-300\,mV\,dec^{-1}$ [31]. In the present case the possible structure of surface oxide and the rate of its transformation by polarization is probably the main reason for the observed differences in Tafel slope values.

4. Conclusions

Oxygen reduction on AISI 304 stainless steel electrodes in a 0.5 M NaCl solution at pH ranging from 4 to 10 proceeds via a four-electron pathway to OH^-. The reaction order with respect to oxygen is unity.

The observed Tafel slopes range from -115 to $-180\,mV\,dec^{-1}$. Cyclic voltammograms performed in an oxygen-free solution show that the Tafel line lies in the potential range where the formation and reduction of Fe(II) and Fe(III) species on the inner Cr_2O_3 rich layer is possible. The electrode coverage (composition and structure), depends on solution pH and scan direction, and this is probably the main reason for the observed differences in Tafel slope.

Well-defined limiting currents were observed in all cases.

References

[1] M. R. Tarasevich, A. Sadkowski and E. Yeager, *in* 'Comprehensive Treatise in Electrochemistry', Vol. 7, (edited by B. E. Conway, J. O'M. Bockris, E. Yeager, S. U. M. Khan and R. E. White), Plenum Press, New York (1983).
[2] F. van den Brink, E. Barendrecht and W. Visscher, *Recueil* **99** (1980) 253.
[3] E. Yeager, *Electrochim. Acta* **29** (1984) 1527.
[4] P. Delahay, *J. Electrochem. Soc.* **97** (1950) 205.
[5] V. Jovancicevic and J. O'M. Bockris, *ibid.* **133** (1986) 1797.
[6] S. Zecevic, D. M. Drazic and S. Gojkovic, *J. Serb. Chem. Soc.* **52** (1987) 649.
[7] S. Zecevic, D. M. Drazic and S. Gojkovic, *J. Electroanal. Chem.* **265** (1989) 179.
[8] S. Zecevic, D. M. Drazic and S. Gojkovic, *Corros. Sci.* **32** (1991) 563.
[9] E. J. Calvo and D. J. Schiffrin, *J. Electroanal. Chem.* **243** (1988) 171.
[10] D. M. Drazic and S. K. Gojkovic, 36th ISE Meeting, Salamanca (1985), Ext. Abs., p. 05050.
[11] D. M. Drazic, S. K. Zecevic and S. Lj. Gojkovic, 38th ISE Meeting, Maastricht (1987), Ext. Abs., p. 678.
[12] H. S. Wroblowa and S. B. Qaderi, *J. Electroanal. Chem.* **279** (1990) 231.
[13] V. A. Kuznetcov and I. P. Nelaev, *Khim. Khim. Tekhnol.* **27** (1984) 206.
[14] A. Bonnel, F. Dabosi, C. Deslouis, M. Dupart, M. Kedam and B. Tribollet, *J. Electrochem. Soc.* **130** (1983) 753.
[15] S. Muralidharan, R. Ravi, G. Rajagopal, N. Palaniswamy and K. Balakrishnan, *in* 'Proceedings of 10th ICMC', Madras (1987) p. 543.
[16] I. Olefjord, B. Brox and U. Jelvestam, *J. Electrochem. Soc.* **132** (1985) 2854.
[17] M. Metikos-Hukovic and M. Ceraj-Ceric, *ibid.* **134** (1987) 2193.
[18] Z. Szklarska-Smialowska, Pitting Corrosion of Metals, NACE publication, Houston, TX (1986).
[19] M. Metikos-Hukovic and I. Milosev, *J. Appl. Electrochem.* **22** (1992) 448.
[20] C. Pallotta, N. de Cristofaro, R. C. Salvarezza and A. J. Arvia, *Electrochim. Acta* **31** (1986) 1265.
[21] R. C. Salvarezza, N. de Cristofaro, C. Pallotta and A. J. Arvia, *ibid.* **32** (1987) 1049.
[22] M. Urretabizkaya, C. D. Pallotta, N. de Cristofaro, R. C. Salvarezza and A. J. Arvia, *ibid.* **33** (1988) 1645.
[23] N. Ramasubramanian, N. Preocanin and R. D. Davidson, *J. Electrochem. Soc.* **132** (1985) 793.
[24] U. Konig and J. W. Schultze, *Werkst. Korros.* **39** (1988) 595.
[25] S. Matsuda, K. Sugimoto and Y. Sawada, *in* 'Passivity of Metals', (edited by R. P. Frankenthal and J. Kruger), The Electrochemical Society, Princeton, NJ (1978) p. 1699.
[26] E. Cavalcanti, G. E. Thompson, G. C. Wood and J. L. Dawson, *in* 'Proceedings of the 9th ICMC', Vol. 4, Toronto (1984) p. 36.
[27] M. G. S. Ferreira and J. L. Dawson, *J. Electrochem. Soc.* **132** (1985) 760.
[28] P. C. Searson and R. M. Latanison, *Electrochim. Acta* **35** (1990) 445.
[29] Yu. V. Pleskov and V. Yu. Filinovskii, 'The Rotating Disc Electrode', Consultant Bureau, New York (1976) p. 91.
[30] H. Abd El-Kader and S. M. El-Raghy, *Electrochim. Acta* **30** (1985) 841.
[31] N. A. Anastasijevic, Z. M. Dimitrijevic and R. R. Adzic, *J. Electroanal. Chem.* **199** (1986) 351.